Journal of Photochemistry and Photobiology A: Chemistry 293 (2014) 32–39

Contents lists available at ScienceDirect

Journal of Photochemistry and Photobiology A: Chemistry

journal homepage: www.elsevier.com/locate/jphotochem

Photochemical behavior of Safranine-Riboflavin complex in the degradation of folic acid

Willy G. Santos*, Regina S. Scurachio, Daniel R. Cardoso

Instituto de Química de São Carlos, Universidade de São Paulo, Av. Trabalhador São Carlense, 400 CP 780, 13560-970, São Carlos, SP, Brazil

ARTICLE INFO

Article history:
Received 5 April 2014
Received in revised form 2 July 2014
Accepted 19 July 2014
Available online 1 August 2014

Keywords:
Dyes
Riboflavin
Safranine
Folic acid
Photochemistry
Electron transfer

ABSTRACT

The photochemistry of safranine complexed with riboflavin and the photoinduced electron transfer from folic acid to the complex were investigated by steady-state and time resolved absorption spectroscopy, and the photoproducts were further analyzed by LC-orbitrap–FT–MS. UV–vis spectra of the complex showed a decrease in the safranine band at 520 nm with increasing concentration of riboflavin, which was attributed to complex formation. A 1:1 (safranine:riboflavin) stoichiometry was determined using Job's method. Following safranine photoexcitation, there is formation of a radical pair in the complex by donation of an electron from ground-state riboflavin to excited-state safranine. The cation radical of riboflavin within this complex reacts with folic acid to yield $FA^{+\bullet}$, which may accept an electron from the anion radical of safranine, avoiding the photobleaching of the safranine. In contrast, the reaction of the anion radical of non-complexed safranine with folic acid leads to safranine photobleaching.

1. Introduction

Safranine is a dye, classified as phenazine derivative, which is widely used in the textile, pharmaceutical, paper and cosmetic industries [1,2]. In addition, safranine finds application in many areas of research, such as biological stain [3,4], electropolymer film synthesis [5,6], and clinical and medicinal application as bio-probe for determination of hyaluronic acid, inhibition of human ribonucleotide reductase, detection of double stranded DNA, molecular adhesive for protein immobilization, as probe for membrane organization, and in several other application [7,8]. This molecule is also employed as a photosensitizer for various chemical reactions [9–11].

In the presence of appropriate molecule, safranine in its triplet-state may accept or donate electron to form the reduced or oxidized species, respectively. The electron transfer between dyes and other redox active compounds is especially suited to studies with model membranes and micelles [12–14]. These reactions play an important role in understanding the molecular mechanism of drug toxicity and the effect of the presence of dyes in cell membrane [15–20].

In recent developments of pharmaceuticals, some organic functional dyes have been shown considerable potential for drug development [21]. In particular, photosensitizer fluorochromes with low toxicity and high photochemical activity, such as flavins, have been widely used in tumor treatment [22] and inactivation of virus in plasma [23]. Riboflavin (Rib) is a relevant photosensitive fluorochrome which is also known as water-soluble Vitamin B_2. In biochemistry, flavin molecules may interact easily with biological macromolecule due to its planar structure. For instance, riboflavin is used as fluorescent probe in the analysis of deoxyribonucleic acid (DNA) [12,24,25].

Electron-transfer reactions from excited-states of dyes represent an important route to produce radicals that might induce various chemical or biological processes. Therefore, the choice of appropriate components for participating in such electron transfer reactions is important, and is a subject of continuous research. After efficiently receiving or donating an electron, these compounds should be able to form reactive radicals or radical ions, either directly or through fragmentation. However, the interaction of safranine and riboflavin was not investigated in detail. The photochemical study with these two sensitizers is important because they can be developed as therapeutic agents.

Concerning the dyes repair mechanism, this work report the electron transfer mechanism of isolated dyes and the complexed dyes with folic acid. The photosensitized mechanism of safranine–riboflavin complex toward folic acid and the dyes repair were studied in detail by direct observation of the transient species

* Corresponding author. Tel.: +55 1633739976.
E-mail addresses: willy_glen@yahoo.com.br, willygsantos@gmail.com (W.G. Santos).

http://dx.doi.org/10.1016/j.jphotochem.2014.07.010
1010-6030/

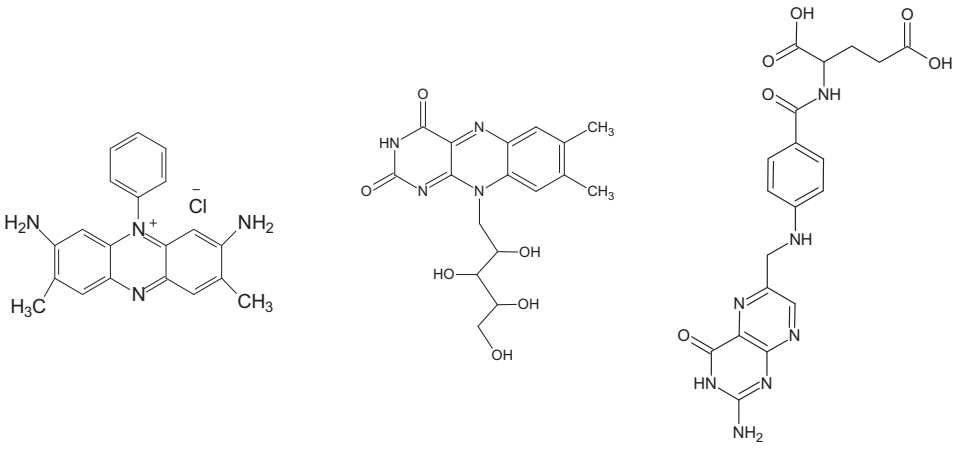

Scheme 1. Chemical structure of the compounds studied.

and their reaction kinetics using time resolved laser flash photolysis technique. The aim of this study was to gain further insight into the photosensitized mechanism of the complex with promising applications for photoinduced electron transfer in biological system.

2. Experimental

2.1. Chemicals

Safranine O 97% (3.7-diamino-2.8-dimethyl-5-phenylphenazinium chloride), riboflavin (Vitamin B_2) and folic acid 97% (Pteroyl-L-glutamic acid or Vitamin B_9) were purchased from Sigma-Aldrich (Steinheim, Germany) and used without further purification. Stock solutions of safranine (10^{-2} mol L^{-1}) and riboflavin (10^{-3} mol L^{-1}) were prepared in buffer solution at 298 K and pH 7.4 (Scheme 1).

2.2. Spectroscopic measurements

Absorption spectra at different temperatures were recorded on a Multskan Go Reader (Thermo Scientific, Waltham MA, US) spectrometer using a 1×1 cm quartz cuvette. In photolysis experiments, the absorption was taken at different irradiation times at 298 K, using a light emitting diode as a light source at 532 nm ± 25 nm filtered by an interferometer at 520 nm ± 5 nm.

Steady-state fluorescence measurements were made on a Hitachi model F4500 (Hitachi-Hitech, Tokyo, Japan) spectrometer equipped with a thermostat for the quenching studies at different temperatures.

Transient absorption spectra were obtained using a LFP-112 Luzchem nanosecond laser flash photolysis spectrometer (Luzchem research, Ottawa, Canada). Excitation of the samples was performed with the third harmonic (355 nm) of a Brio Nd-YAG laser (Quantel, Les Ulis, France), with 5.2 ns light pulses and power of 10 mJ cm^{-2}. Kinetic analyses were made with the Luzchem proprietary software.

2.3. Potassium ferrioxalate actinometry

The absorbance of 0.15 mol L^{-1} solution of $K_3[Fe(C_2O_4)_3]$ was measured at 550 nm, measured before and after the solution was irradiated for 20 min at 20 °C, to determine the fraction of light absorbed. The number of moles of ferrous ion produced upon light irradiation was then determined by measuring the amount of $[Fe(phenanthroline)_3]^{2+}$ formed after addition of phenanthroline. This procedure was accomplished by adding 1 mL of photolyzed sample, 0.5 mL of acetate buffer (600 mL of 1 mol L^{-1} sodium acetate and 360 mL 0.5 mol L^{-1} H_2SO_4 diluted to a total volume of 1 L), and 2 mL of a 0.1% aqueous phenanthroline solution to 10 mL of water. After standing for 15 min in the dark, the amount of $[Fe(phenanthroline)_3]^{2+}$ was determined by measuring the absorbance at 510 nm (ε = 11,100 L mol^{-1} cm^{-1}). The procedure was repeated with a sample of ferrioxalate kept in the dark. Five independent runs were averaged to determine the intensity of light incident on the sample. The absorbance measurements were carried out employing a Hitachi U-3501 (Hitachi-Hitech, Tokyo, Japan) spectrophotometer.

2.4. Liquid chromatography accurate ultra-high resolution mass spectrometry

LC–MS/MS analyses were carried out using an LTQ Orbitrap Velos FT-MS mass spectrometer (Thermo Fischer Scientific, Bremen, Germany) with a UPLC Thermo Scientific model Accela LC Systems. 5 μL of the sample was injected onto a Waters Spherisorb S5 C18 reverse phase column (2 mm × 250 mm × 4.6 μm) maintained at 40 C. A constant flow rate of 0.3 mL min^{-1} was used with the following gradient: 15% B isocratic for 20 min, then up to 90% B for 10 min and 15% B for 5 min. Solvent A was 0.1% formic acid in water and solvent B was 0.1% formic acid in acetonitrile. The final composition was analyzed by direct infusion into an HESI interface ionization (Thermo Scientific, Bremen, Germany).

3. Results and discussion

3.1. Ground-state and singlet-state process

The complex between riboflavin (Rib) and safranine (Saf) was first studied by steady-state UV–vis absorption spectroscopy. Fig. 1a shows the absorption spectrum of riboflavin that presents absorption maxima at 373 nm and 440 nm. The safranine absorption has a maximum centered at 520 nm, which is decreased upon addition of riboflavin.

The Job's plot shown in Fig. 1b presents the ratio of absorbance between the riboflavin measured at 373 nm and safranine at 520 nm at different volume ratios, considering the concentration of each stock solutions ([Sf] = 1×10^{-5} mol L^{-1}; [Rib] = 1×10^{-4} mol L^{-1}) at different proportional volumes. The absorbance ratio initially increases upon complex formation and

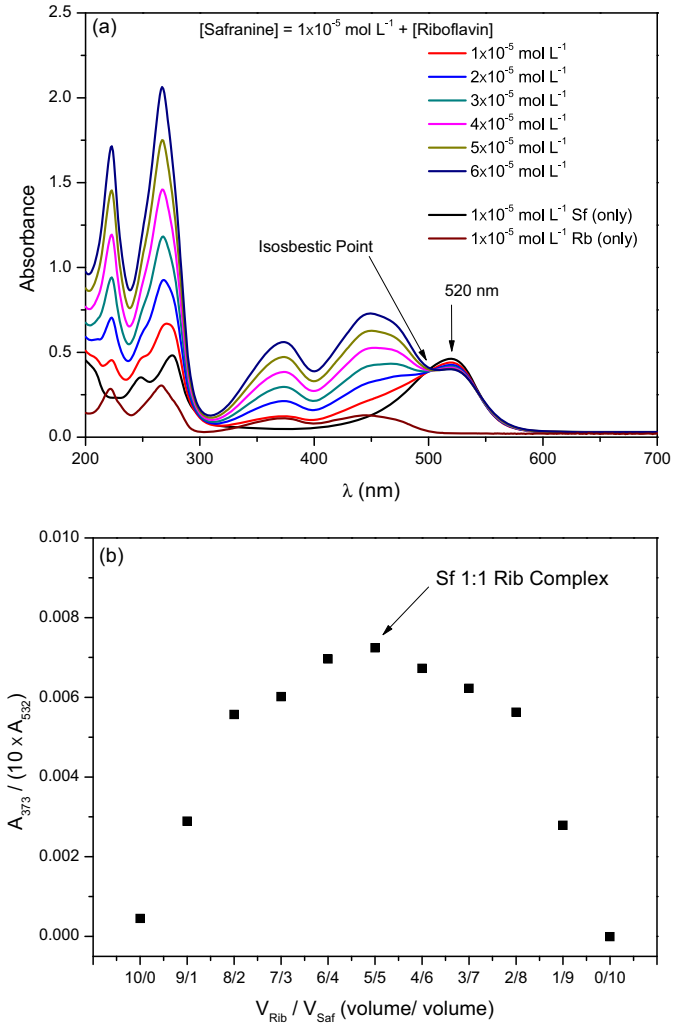

Fig. 1. (a) Absorption spectra of safranine in the presence and absence of riboflavin. (b) Job's plot for the Sf–Rib complex in aqueous buffer solution at pH 7.4 and 298 K.

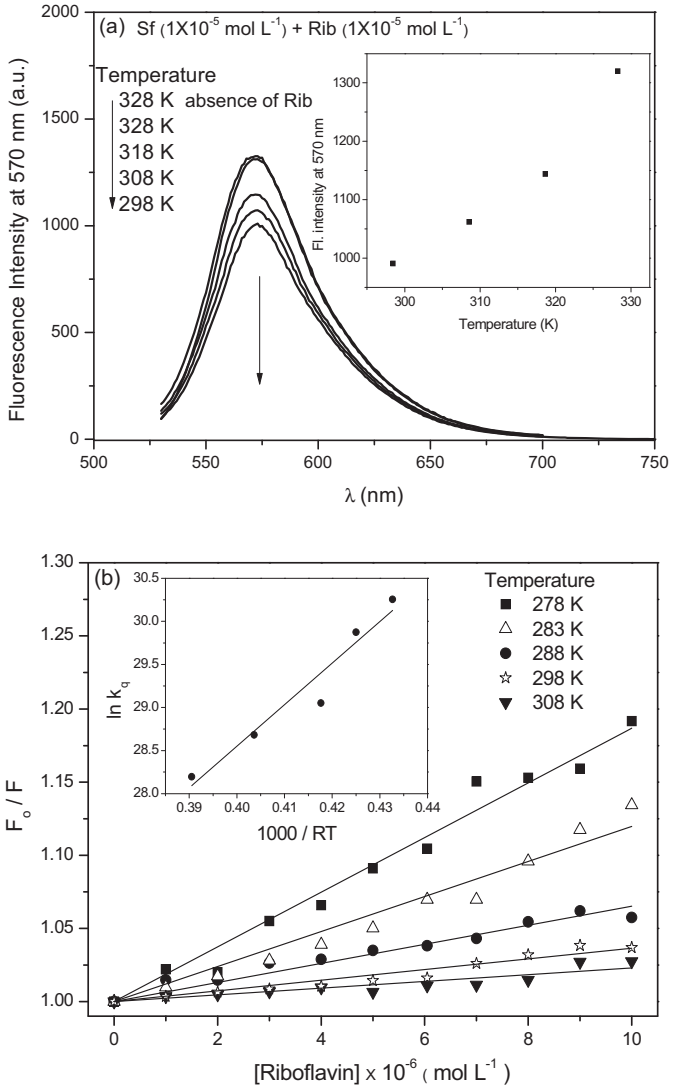

Fig. 2. (a) Fluorescence spectra and (b) Stern–Volmer plot for Sf + Rib system in aqueous buffer solution at pH 7.4 and at different temperatures. Inset (a): Fluorescence intensity of safranine at different temperatures. Inset (b): Rate constant for the quenching of safranine fluorescence recorded at different temperatures. λ_{exc} = 520 nm; λ_{em} = 570 nm.

subsequently decreases with further safranine addition. The maximum value of absorbance ratio in the Job's plot (Fig. 1b) shows a stoichiometry of 1:1 (Rib:Sf) for the dominant species.

The fluorescence emission of safranine has a maximum centered at 570 nm, which is quenched in presence of increasing concentration of riboflavin, as may be observed in Fig. 2a and b.

The high fluorescence quenching constant ($^1k_q = 2.86 \pm 0.21 \times 10^{12}\,\mathrm{L\,mol^{-1}\,s^{-1}}$) at 298 K is faster than the diffusion controlled rate, and suggest that the process is likely to be dominated by a static quenching rather than a dynamic quenching. In fact, in agreement with this measurements using time resolved fluorescence measurements were carried and no changes were observed for the safranine time-decay ($\tau_F = 1.40 \pm 0.02$ ns at 298 K). However, in the situation of complex formation, fast fluorescence quenching may be possible and proportional to a complex quantity. Fig. 2b inset shows the fluorescence quenching constant of safranine in presence of riboflavin recorded at different temperatures.

Since the complex (Sf–Rib) does not present any absorption in the region of the safranine spectrum, the concentration of complex may be calculated in terms of the depletion of safranine absorption at 520 nm, see Fig. 1a. Assuming [Sf–Rib] < [Sf] or [Rib], we may write the following equation as

$$A_o - A_i = K_{eq} \times \varepsilon_o \times d \times [\mathrm{Sf}]^m \times [\mathrm{Rib}]^n \quad (1)$$

where A_o and A_i are the safranine absorption at 520 nm in the absence and presence of riboflavin, m and n represent the stoichiometric indices for safranine and riboflavin, respectively. The extinction coefficient (ε_o) for safranine in the ground-state is $4.8 \pm 0.23 \times 10^4\,\mathrm{L\,mol^{-1}\,cm^{-1}}$ and d is the optical path of cell used for absorbance measurements.

To evaluate the coefficients m and n coefficients in Eq. (1), data from the measurement of the formation constant of the complex were used. The values of both m and n are nearly unit, considering a 1:1 stoichiometry for the complex. The equilibrium constant value ($K_{eq} = 1.6 \pm 0.1 \times 10^4\,\mathrm{L\,mol^{-1}}$ at 298 K) was determined in high concentrations of riboflavin, assuming that the concentration of riboflavin does not change significantly upon complexation, since [Rib] ≫ [Sf]. The effect of temperature on the equilibrium is shown in Fig. 3.

From the angular coefficient in Fig. 3 (inset) and the Van't Hoff equation (Eq. (2)), the enthalpy of complex formation can be calculated, and has the value $\Delta H^\circ = 50.5 \pm 0.8\,\mathrm{kJ\,mol^{-1}}$. The same value of ΔH° was found for all three curves in Fig. 3 (inset).

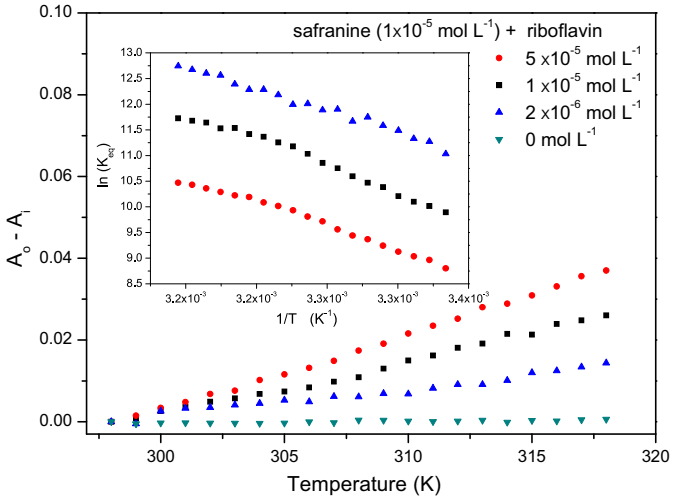

Fig. 3. Difference spectra for safranine absorption in the absence and presence of riboflavin at different temperatures. Inset: Van't Hoff plot for the equilibrium of safranine–riboflavin complexation in aqueous buffer at pH = 7.4. λ_{obs} = 520 nm.

$$\ln\left(K_{eq}\right) = \frac{\Delta S^o}{R} - \frac{\Delta H^o}{RT} \quad (2)$$

The value of ΔS° was estimated from the intercept point, relating values <4 J K^{-1} mol^{-1} for all curves, which is strongly dependent on the free safranine and riboflavin in solution. In agreement with the thermodynamic values obtained for absorption measurements, the enthalpy found for fluorescence measurements at 570 nm, in Fig. 2 (inset), has $\Delta H^\circ = 48.7 \pm 0.7$ kJ mol^{-1} and $\Delta S^\circ = 9 \pm 0.4$ J K^{-1} mol^{-1}.

The value of Gibbs free energy was calculated from the following equation:

$$\Delta G^o = -RT \ln\left(K_{eq}\right) \quad (3)$$

The high negative value of Gibbs free energy (-50.1 kJ $\pm$ 1.2 mol^{-1}) compared with entropy indicates a favorable formation of Sf–Rib complex for all concentration of safranine and riboflavin and that the formation is mainly due to hydrophobic interaction.

3.2. Triplet state process

Following excitation with a 532 nm laser pulse in deaereated buffer solution at pH 7.4, safranine shows transient absorptions centered at 300, 400, 650 and 810 nm, as shown in Fig. 4a. No transients are observed in air saturated solutions. At pH 7.4, the major peak of the triplet state of safranine may be seen at 810 nm, and is observed over the whole spectral range to decay with the lifetime of 18 μs at 298 K.

In the absence of quenchers the triplet excited state decays by a first order kinetics due to a self-quenching process [10,11,26,27], leading to long lifetime absorption at 400 nm and 650 nm that are attributed to the triplet and semireduced form of the safranine with a lifetime of 100–200 μs at 298 K in aqueous buffer pH 7.5. The semioxidized form of safranine is observed at 440 nm with lifetime of 30–40 μs, and is formed by the same self-quenching reaction

$$^3\mathrm{Sf} + \mathrm{Sf} \rightarrow \mathrm{Sf}^{+\bullet} + \mathrm{Sf}^{-\bullet}$$

The lifetime and absorption band of the semireduced and oxidized radical of safranine were observed in our previous work [10,11].

In this self-quenching mechanism, it is very difficult to distinguish the semioxidized safranine kinetics from the triplet–triplet decay due to very similar lifetimes.

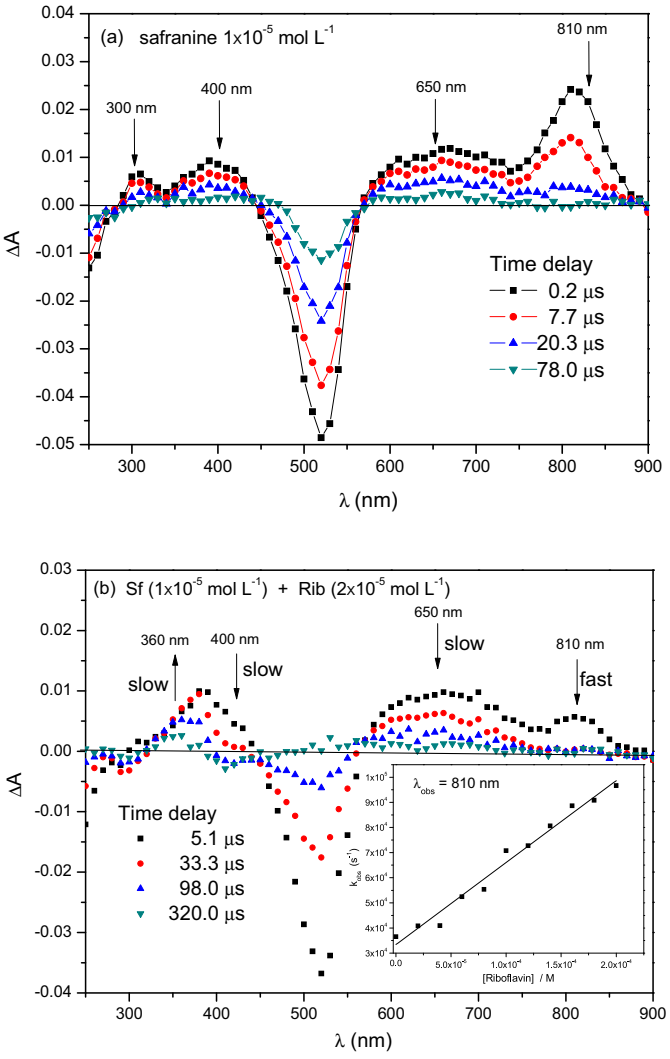

Fig. 4. Transient absorption spectrum of safranine in aqueous solution at pH 7.4 and recorded at different times after laser pulse, in the (a) absence and (b) presence of riboflavin. Inset: Observed pseudo first-order rate constant as function of riboflavin concentration. λ_{exc} = 532 nm and power of 16 mJ cm^{-2}.

In the presence of riboflavin, the triplet state of safranine is quenched, and, as observed 98 μs after the laser pulse, there is, simultaneously, an increase in the absorption at 360 nm and absorption depletion at 400–420 nm and 600–700 nm, indicating an increase in the amount of semireduced form of safranine and within the same lifetime range as has been observed with safranine in the presence of other electron donors [11,27]. This may suggests that electron transfer between riboflavin and safranine triplet state, yield the semireduced form of safranine and the semioxidized cation radical of riboflavin.

$$^3\mathrm{Sf} + \mathrm{Rib} \rightarrow \mathrm{Sf}^{-\bullet} + \mathrm{Rib}^{+\bullet}$$

The radical cations of various flavins has been ascribed previously by P.F. Heelis and co-workers to have absorption bands in the 300–450 nm and 600–650 nm regions, and to decay by first order kinetics, with $k_1 = 10^3$ s^{-1} and 10^4 s^{-1} at pH = 4 and 9, respectively [28]. This rate constant is in agreement with our species observed at 360 nm with $k_1 = 2.47 \pm 0.03 \times 10^3$ s^{-1} at 298 K and pH 7.5. Fig. 5 shows the kinetic decays of the various transient species.

The second-order rate constant for the quenching of ^{3}Saf by Rib ($3.3 \pm 0.1 \times 10^8$ L mol^{-1} s^{-1}) was determined from safranine lifetime at 810 nm (Fig. 4b inset). This is lower than the diffusion limit

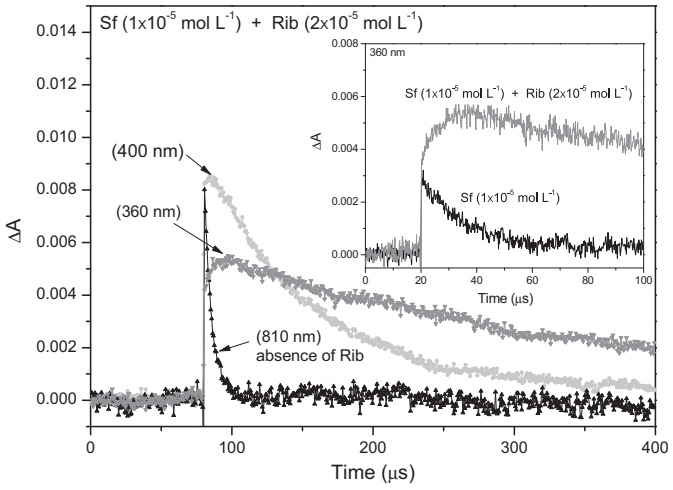

Fig. 5. Kinetic traces for different transient decays monitored in real-time at various wavelength following laser pulses of 10 mJ cm^{-2} at 532 nm in argon-saturated buffer solution at pH 7.4 and 298 K. Inset: Triplet-decay of safranine and transient growth of the riboflavion cation radical, both observed at 360 nm.

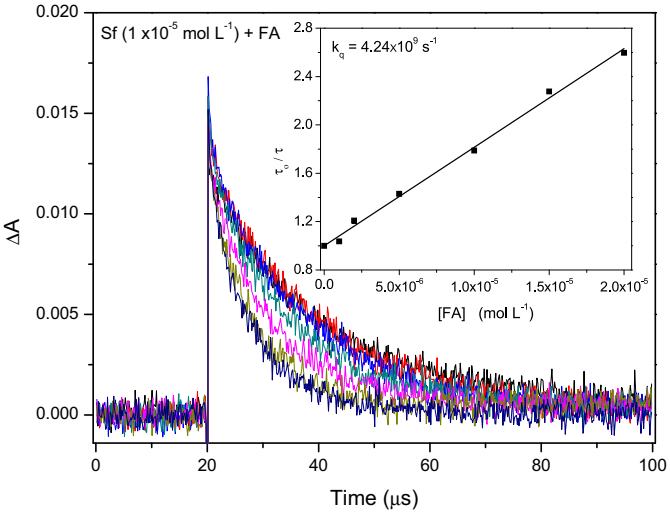

Fig. 6. Kinetic traces for triplet-excited safranine decay monitored in real-time at 810 nm following laser pulses of 10 mJ cm^{-2} at 532 nm for increasing concentrations of folic acid in argon-saturated buffer solution at pH 7.4 and 298 K. Inset: observed pseudo first-order rate constant as function of folic acid concentration.

in aqueous solution (10^{10} L mol^{-1} s^{-1}), in contrast with what is frequently observed with bimolecular deactivation of triplet-states.

In the presence of folic acid, the triplet of safranine is quenched with lifetime of 100 μs, and is accompanied by an increase in absorption in the 400–450 nm region and other at 600–700 nm. These absorptions have been ascribed to semireduced form of safranine [11,27], which is formed by an electron transfer from the folic acid to the safranine triplet state.

$$^3Sf + FA \rightarrow Sf^{-\bullet} + FA^{+\bullet}$$

The addition of folic acid to safranine solution quenches the triplet absorption of non-complexed safranine with $k_q = 4.29 \pm 0.08 \times 10^9$ L mol^{-1} s^{-1} at 298 K (Fig. 6). The lifetime of the cation radical of folic acid is very short, and it rapidly decomposes to form secondary products (pterin-6-carboxylic, *p*-aminobenzoyl-L-glutamic acid and the oxaziridine derivative) [29–32].

When the folic acid is added in the Saf–Rib complex solution, the rate of growth of the cation radical absorption at 360 nm is slower than with Saf–Rib complex alone, as may be seen in Fig. 7.

The differences in the rate of growth of the transient suggest complex competitive process of quenching of safranine by FA and by riboflavin, which is characterized by an increase in the solution. The low depletion of the absorption supports this idea, since reaction of the cation radical of riboflavin with FA should deplete all the absorption of the radical species, which is not observed in Fig. 7 at high concentrations of FA.

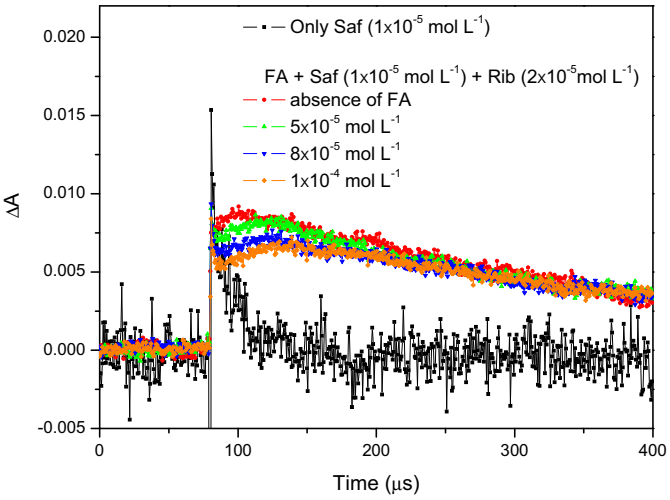

Fig. 7. Kinetic traces for radical cation formation of riboflavin monitored in real-time at 360 nm following laser pulses of 10 mJ cm^{-2} at 532 nm for increasing concentrations of folic acid in argon-saturated buffer solution at pH 7.4 and 298 K.

3.3. Photobleaching process

The photolysis of the Sf–Rib system was carried out by exciting the safranine absorption band at 520 nm, in degassed aqueous buffer pH 7.4 solutions. Fig. 8a and b shows the absorption behavior

Table 1
Photobleaching rate constant for systems containing safranine, riboflavin and folic acid in aqueous buffer solution at 298 K and pH 7.4.

[Safranine] (mol L^{-1})	[Riboflavin] (mol L^{-1})	[Folic acid] (mol L^{-1})	$k_{PB} \times 10^2$ min^{-1}	Φ_{PB}
1×10^{-5}	–	–	1.01	0.026
3×10^{-5}	–	–	1.12	0.029
5×10^{-5}	–	–	1.41	0.036
1×10^{-5}	5×10^{-6}	–	1.22	0.031
1×10^{-5}	1×10^{-5}	–	1.65	0.042
1×10^{-5}	3×10^{-5}	–	2.38	0.061
1×10^{-5}	–	1×10^{-6}	2.85	0.078
1×10^{-5}	3×10^{-5}	1×10^{-6}	1.90	0.049
1×10^{-5}	3×10^{-5}	5×10^{-6}	0.82	0.021
1×10^{-5}	3×10^{-5}	1×10^{-5}	0.03	0.001
1×10^{-5}	3×10^{-5}	5×10^{-5}	$<10^{-3}$	–

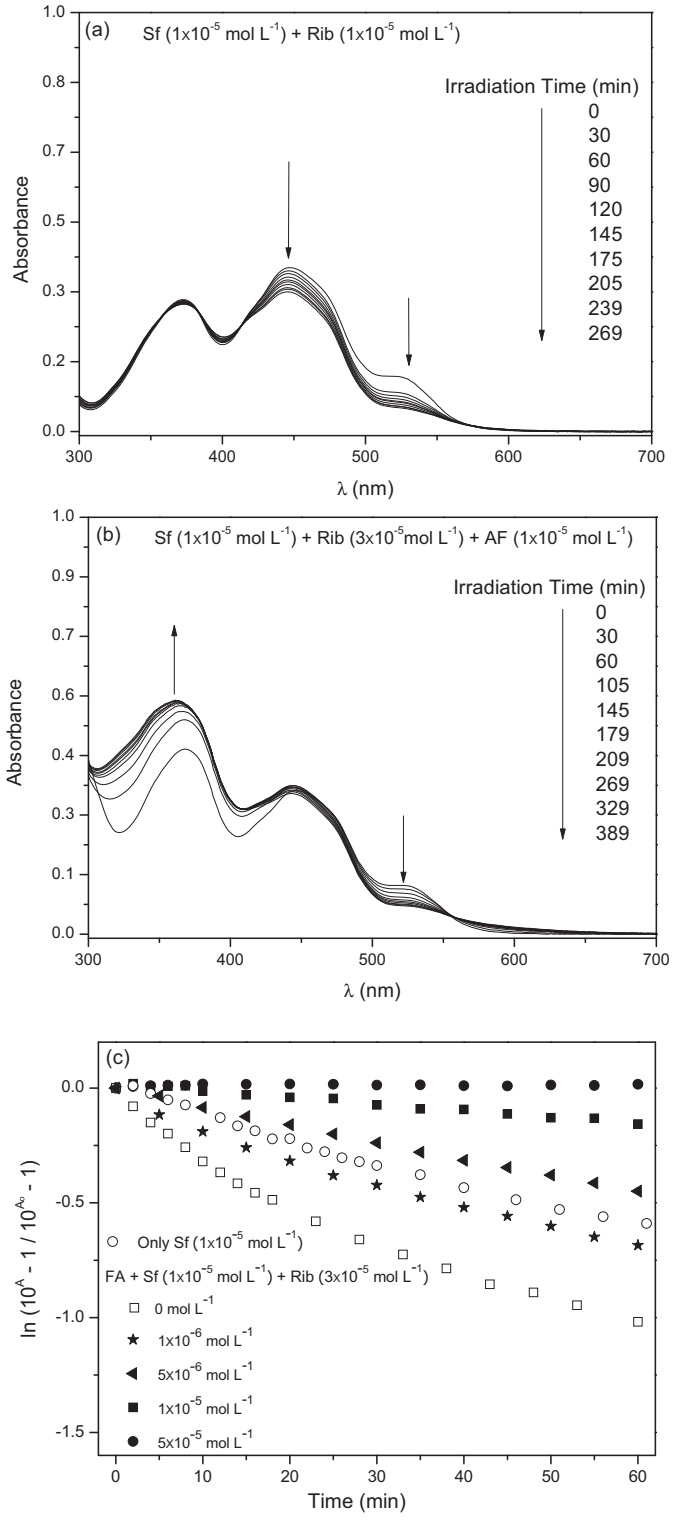

Fig. 8. Absorption spectra of (a) safranine/riboflavin and (b) safranine/riboflavin/folic acid systems after different times of irradiation; (c) photobleaching of safranine alone and in complex form, in the presence and absence of folic acid at 298 K and pH = 7.4.

of the safranine/riboflavin and complex/FA solutions in different times of irradiation. The kinetic properties were studied by monitoring the absorption band of the safranine at different irradiation times. The rate of photobleaching is given by Eq. (4) [11,33]

$$\ln \frac{10^{A} - 1}{10^{A_o} - 1} = -\varepsilon \times I_o \times d \times \Phi_{PB} \times t = k_{PB} \times t \quad (4)$$

where Φ_{PB} is the photobleaching quantum yield, A is the absorbance due to the complex absorption, A_o is the safranine absorption in the absence of riboflavin, ε is the molar absorption coefficient at the irradiation wavelength, d is the irradiation path length and I_o is the light source intensity at 520 nm.

From the slopes of the plots in Fig. 8c, and using Parker ferrioxalate actinometer for the determination of the incident light flux ($I_o = 8.68 \times 10^8$ E min^{-1}), the photobleaching quantum yields were determined and compared for different chemical systems, as shown in Table 1. It may be seen that the presence of riboflavin or FA in the safranine solution increases the photobleaching of the safranine. However, when folic acid is added to the Sf–Rib complex solution, the safranine photobleaching is decreased and its proportional to the folic acid concentration.

The more effective photobleaching observed for Sf/FA in comparison with the Sf–Rib complex supports the results obtained for quenching of the triplet-state of safranine, where the FA is seen to quench safranine ten times faster than Sf–Rib complex.

The proposed mechanism, considering all photochemical studied in this work, is presented in Scheme 2.

3.4. Photoproducts of folic acid sensitized by safranine

Photoreaction was studied of mixtures containing safranine (5×10^{-5} mol L^{-1}) and folic acid (5×10^{-4} mol L^{-1}) in aqueous phosphate buffer solution (pH 7.4, $I = 0.1$ mol L^{-1} NaCl at 298 K). High resolution accurate mass spectra, recorded in the positive ion mode, show characteristic profiles consisting of peaks attributable to safranine, folic acid and three main photoproducts derived from folic acid. These photoproducts display different retention times (1) $tr = 5.49$ min ($[M+H]^+ = 192.05112$ $m/z \pm 2.5$ ppm, as calculated for $C_7H_6O_2N_5$ and assigned as 6-formylpterin); (2) $tr = 5.87$ min ($[M+H]^+ = 267.09717$ m/z ±1.4 ppm, as calculated for $C_{12}H_{15}O_5N_2$ and assigned as *p*-aminobenzoylglutamate moiety released from the pterin), and (3) $tr = 7.68$ min ($[M+H]^+ = 456.12506$ m/z ±2.5 ppm, as calculated for $C_{19}H_{18}O_7N_7$ and assigned as a folic acid oxaziridine derivative). The same photoproducts obtained for Sf/FA chemical system have previously been observed by Scurachio and co-workers [29], in the riboflavin is used as sensitization agent for folic acid degradation [34–44].

Results with Sf–Rib complex in presence of folic acid show the same peaks as in Sf/FA system. However, in the equilibrium situation, the riboflavin and safranine in non-complex make it impossible to identify the effective participation of the complex in folic acid degradation.

The photoproducts of the photolysis of Saf–Rib/FA system at 532 nm for 1 h30 min were characterized and identified by high-resolution accurate mass spectroscopy in the positive mode. The photoproducts were tentatively assigned to 6-formylpterin, *p*-aminobenzoyl-L-glutamic acid and oxaziridine derivative, respectively. These same mass spectrometry characterizations were obtained by others researchers upon irradiating riboflavin in the presence of folic acid [29–32]. The proposed mechanism of the photoproducts generation by complex sensitization is shown in Scheme 3.

The products of the safranine and complex-induced photooxidation of folic acid corroborate to understand the nature of photo reaction and identify a new photochemical method to avoid the riboflavin degradation.

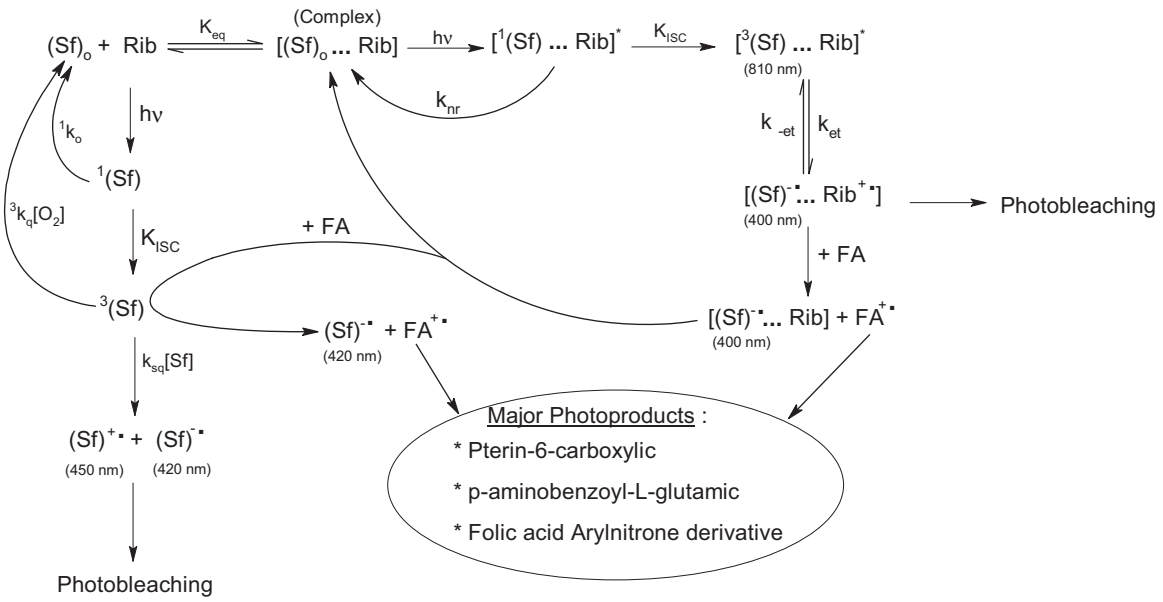

Scheme 2. Proposed photochemical mechanism for Sf–Rib complex reactions in the presence and absence of FA.

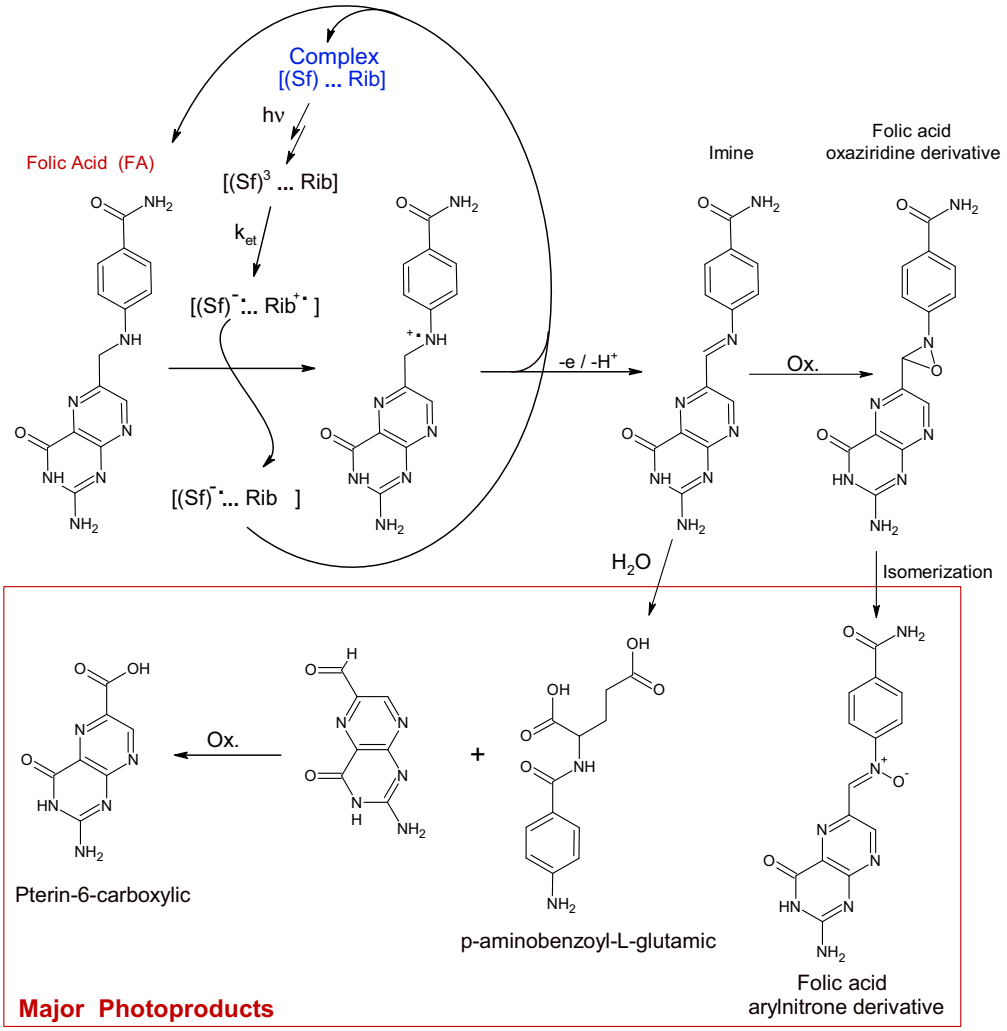

Scheme 3. Proposed mechanism for the generation of folic acid photoproducts.

4. Conclusion

Absorption and fluorescence spectra indicate the formation of a complex between safranine and riboflavin in the ground-state with stoichiometry 1:1 (Rib:Sf) for the dominant species. The equilibrium constant and others thermodynamic parameters ($K_{eq} = 1.6 \pm 0.1 \times 10^4\ L\ mol^{-1}$, $\Delta H^\circ = 48.7 \pm 0.7\ kJ\ mol^{-1}$, $\Delta S^\circ = 9 \pm 0.4\ J\ K^{-1}\ mol^{-1}$ and $\Delta G^\circ = -50.1 \pm 1.2\ kJ\ mol^{-1}$ at 298 K) were obtained by our formulated equation (Eq. (1)) and Van't Hoff equation. In the complex form, the excited dye safranine accepts an electron from riboflavin, forming the very reactive cation radical of riboflavin and the semireduced form of the safranine. The riboflavin cation radical decays by first order kinetics, with $k_1 = 2.47 \pm 0.03 \times 10^3\ s^{-1}$. Excitation at 532 nm (in the safranine absorption band) of deareated solutions of Saf/Rib complex leads to formation of the safranine triplet state, absorbing at 810 nm, which decays to form two transient band at 360 nm and 650 nm, attributed to riboflavin cation radical and the semireduced form of safranine radical, respectively. Folic acid quenches safranine triplet state by an electron transfer process ($k_q = 4.29 \pm 0.08 \times 10^9\ L\ mol^{-1}\ s^{-1}$). When the folic acid is added in the Saf–Rib complex solution, the lifetime of radical growth is slower than with the Saf–Rib complex alone, indicating a competitive process between safranine and Saf/Rib to react with FA. This conclusion is supported by photobleaching experiments, where the increases of the folic acid concentration decrease the safranine bleaching.

Acknowledgements

This work was supported by São Paulo Research Foundation—FAPESP (grants 2012/19823-4, 2011/57555-7 and 2009/54040-8).

References

[1] D.F. Eaton, Adv. Photochem. 13 (1986) 427–487.
[2] A.D. Ketley, J. Radiat. Curing 19 (1982) 35.
[3] H.W. Gao, J.F. Zhao, J. Trace Microprobe Technol. 21 (2003) 615–625.
[4] J. Li, Z. Wang, J. Wang, J. Gao, M. Zou, Y. Li, B. Wang, L. Xia, J. Lumin. 132 (2012) 282–288.
[5] R. Pauliukaite, A. Sealskiene, A. Malinauskas, C.M.A. Brett, Thin Solid Films 517 (2009) 5435–5441.
[6] S. Guo, Q. Zhu, B. Yang, J. Wang, B. Ye, Food Chem. 129 (2011) 1311–1314.
[7] D. Bose, D. Ghosh, P. Das, A. Girigoswami, D. Sarkar, N. Chattopadhyay, Chem. Phys. Lipids 163 (2010) 94–101.
[8] E. Bozkurt, T. Bayraktutan, M. Acar, M. Toprak, Spectrochim. Acta, A: Mol. Biomol. Spectrosc. 101 (2013) 31–35.
[9] R. Jain, N. Sharma, N. Jadon, K. Radhapyari, Int. J. Environ. Pollut. 27 (2006) 121–134.
[10] W.G. Santos, T.T. Tominaga, O.R. Nascimento, C.C. Schmitt, M.G. Neumann, J. Photochem. Photobiol. A: Chem. 236 (2012) 14–20.
[11] W.G. Santos, C.C. Schmitt, M.G. Neumann, Photochemistry of tetraphenyldiboroxane and its use as photopolymerization co-initiator, Photochem. Photobiol. 89 (2013) 1362–1367.
[12] S.Y. Bi, C.Y. Qiao, D.Q. Song, Y. Tian, D.J. Gao, Y. Sun, H.Q. Zhang, Sens. Actuators, B: Chem. 19 (2006) 199–208.
[13] A. Murza, S. Sanchez-cortes, J.V. Garcia-Ramos, J.M. Guisan, C. Alfonso, G. Rivas, Biochemistry 39 (2000) 10557–10565.
[14] M.N. Usacheva, M.C. Teichert, M.A. Biel, J. Photochem. Photobiol. B: Biol. 71 (2003) 87–98.
[15] D.T. Cramb, S.C. Beck, J. Photochem. Photobiol. A: Chem. 134 (2000) 87–95.
[16] J.L. Vazquez, M.T. Montero, J. Trias, J. Hernandez-Borrell, Int. J. Pharm. 171 (1998) 75–86.
[17] E. Blatt, R.C. Chatelier, W.H. Sawyer, Biophys. J. 50 (1986) 349–356.
[18] G.M. Omann, M. Glaser, Biophys. J. 47 (1985) 623–627.
[19] S.K. Ghosh, S.C. Bhattacharya, Chem. Phys. Lipids 13 (2004) 151–158.
[20] R. Fato, M. Battino, G.M. Castelli, G. Lenaz, FEBS 179 (1985) 238–242.
[21] M. Wainwright, Dyes Pigm. 76 (2008) 582–589.
[22] M. Wainwright, R.M. Giddens, Dyes Pigm. 57 (2003) 245–257.
[23] H. Mohr, J. Knuver-Hopf, U. Gravemann, A. Redecker-Klein, T.H. Muller, Transfusion 44 (2004) 886–890.
[24] G.M. Zhang, Y.H. Pang, S.M. Shuang, C. Dong, M.M.F. Choi, D.S. Liu, J. Photochem. Photobiol. A: Chem. 169 (2005) 153–158.
[25] Y. Cao, X.W. He, Z. Gao, L. Peng, Talanta 49 (1999) 377–383.
[26] S.G. Bertolotti, C.M. Previtali, J. Photochem. Photobiol. A: Chem. 103 (1997) 115–119.
[27] M.V. Encinas, C.M. Previtali, M.H. Gehlen, M.G. Neumann, J. Photochem. Photobiol. A: Chem. 94 (1996) 237–241.
[28] P.F. Heelis, B.J. Parsons, G.O. Phillips, J. Phys. Chem. 90 (1986) 6833–6836.
[29] R.S. Scurachio, L.H. Skibsted, G. Metzker, D.R. Cardoso, J. Photochem. Photobiol. A: Chem. 87 (2011) 840–845.
[30] M.J. Akhtar, M.A. Khan, I. Ahmad, J. Pharm. Biomed. Anal. 19 (1999) 269–275.
[31] M.J. Akhtar, M.A. Khan, I. Ahmad, J. Pharm. Biomed. Anal. 23 (2000) 1039–1044.
[32] M.J. Akhtar, M.A. Khan, I. Ahmad, J. Pharm. Biomed. Anal. 31 (2003) 579–588.
[33] W.G. Santos, C.C. Schmitt, M.G. Neumann, J. Photochem. Photobiol. A: Chem. 252 (2013) 124–130.
[34] I. Ahmad, H.D.C. Rapson, J. Pharm. Biomed. Anal. 8 (1990) 217–223.
[35] M.J. Akhtar, M.A. Khan, I. Ahmad, J. Photochem. Photobiol. B: Biol. 16 (1997) 95–99.
[36] I. Ahmad, Q. Fasihullah, F.H.M. Vaid, J. Photochem. Photobiol. B: Biol. 75 (2004) 13–20.
[37] I. Ahmad, Q. Fasihullah, F.H.M. Vaid, J. Photochem. Photobiol. B: Biol. 78 (2005) 229–234.
[38] I. Ahmad, Q. Fasihullah, F.H.M. Vaid, J. Photochem. Photobiol. B: Biol. 82 (2006) 21–27.
[39] I. Ahmad, S. Ahmed, M.A. Sheraz, F.H.M. Vaid, J. Photochem. Photobiol. B: Biol. 93 (2008) 82–87.
[40] I. Ahmad, S. Ahmed, M.A. Sheraz, F.H.M. Vaid, Izhar A. Ansari, Int. J. Pharm. 390 (2010) 174–182.
[41] I. Ahmad, M.A. Sheraz, S. Ahmed, S.H. Kazi, T. Mirza, M. Aminuddin, Results Pharm. Sci. 1 (2011) 11–15.
[42] M.A. Sheraz, S.H. Kazi, S. Ahmed, T. Mirza, I. Ahmad, M.P. Evstigneev, J. Photochem. Photobiol. A: Chem. 273 (2014) 17–22.
[43] D.R. Cardoso, R.S. Scurachio, W.G. Santos, P. Homem-de-Mello, L.H. Skibsted, J. Agric. Food. Chem. 61 (2013) 2268–2275.
[44] D.R. Cardoso, K. Olsen, L.H. Skibsted, J. Agric. Food. Chem. 55 (2007) 6285–6291.